PERSPECTIVE

Applications of machine learning in computational nanotechnology

To cite this article: Wenxiang Liu *et al* 2022 *Nanotechnology* **33** 162501

IOP Publishing Nanotechnology
Nanotechnology 33 (2022) 162501 (22pp) https://doi.org/10.1088/1361-6528/ac46d7

Perspective

Applications of machine learning in computational nanotechnology

Wenxiang Liu[1], **Yongqiang Wu**[2], **Yang Hong**[3], **Zhongtao Zhang**[4], **Yanan Yue**[1,*] and **Jingchao Zhang**[5,*]

[1] *Key Laboratory of Hydraulic Machinery Transients (MOE), School of Power and Mechanical Engineering, Wuhan University, Wuhan, Hubei 430072, People's Republic of China*

[2] *Weichai Power CO., Ltd, Weifang 261061, People's Republic of China*

[3] *Research Computing, RCAC, Purdue University, West Lafayette, IN 47907, United States of America*

[4] *Holland Computing Center, University of Nebraska-Lincoln, Lincoln, NE, United States of America*

[5] *NVIDIA AI Technology Center (NVAITC), Santa Clara, CA 95051, United States of America*

E-mail: yyue@whu.edu.cn and jingchaoz@nvidia.com

Published 24 January 2022

Abstract

Machine learning (ML) has gained extensive attention in recent years due to its powerful data analysis capabilities. It has been successfully applied to many fields and helped the researchers to achieve several major theoretical and applied breakthroughs. Some of the notable applications in the field of computational nanotechnology are ML potentials, property prediction, and material discovery. This review summarizes the state-of-the-art research progress in these three fields. ML potentials bridge the efficiency versus accuracy gap between density functional calculations and classical molecular dynamics. For property predictions, ML provides a robust method that eliminates the need for repetitive calculations for different simulation setups. Material design and drug discovery assisted by ML greatly reduce the capital and time investment by orders of magnitude. In this perspective, several common ML potentials and ML models are first introduced. Using these state-of-the-art models, developments in property predictions and material discovery are overviewed. Finally, this paper was concluded with an outlook on future directions of data-driven research activities in computational nanotechnology.

Keywords: machine learning, material discovery, property prediction, artificial neural network potential, molecular dynamics

(Some figures may appear in colour only in the online journal)

Introduction

Machine learning has been used in many different fields and has contributed significantly to the advances of biology [1], medicine [2–5], chemistry [6–13] and materials science [14–19]. In chemistry, the discovery of new and more efficient catalysts is restricted by the need for keen scientific intuition and expensive chemical experiments. A new direction is to help discover and accelerate the search for catalysts through machine learning algorithms [20–24]. Suzuki *et al* [24] used several machine learning methods to predict the multicomponent catalyst performance and explore the catalyst optimization. Twenty promising catalyst candidates were found based on the optimization. In addition, with the development of nanotechnology, new materials are constantly being discovered and explored [25–37]. These pose the more demanding challenges in predicting material properties which require higher precision and faster speed. Machine learning provides a promising solution to satisfy this requirement.

Machine learning has achieved great successes in properties prediction [38–43] and new materials discovery [44–49]. Traditional property prediction is based on the experiments and calculations which are time-consuming and capital intensive. For example, thermal conductivity is an important physical quantity that can characterize the thermal properties of a material. There are many ways to measure thermal conductivity, like the hot wire method [50, 51], 3ω method [52] and laser-flash method [53], etc. Meanwhile, despite new advanced measurement technologies [54–56] being constantly developed but challenges remain,

* Authors to whom any correspondence should be addressed.

especially for low-dimensional materials. Computational methods, such as density functional theory [57, 58] (DFT), Boltzmann transport equation [59–61] (BTE), equilibrium and non-equilibrium molecular dynamics [62–64] can be used to predict the thermal conductivity which can provide more physical insight. However, DFT calculations are extremely costly and time-consuming applied in large-scale systems, while molecular dynamics simulations can be employed in large-scale systems, the accuracy is often poor, so a calculation method that combines the advantages of both is urgently needed.

Common machine learning methods in properties prediction and materials discovery include artificial neural networks [65] (ANN), support vector machines [66] (SVM), decision trees [67], Gaussian process regression [68] (GPR), Bayesian optimization [69], etc. Seko *et al* [70] proposed the descriptors of compound and used different machine learning methods, including kernel ridge regression, Gaussian process regression and Bayesian optimization, to predict the physical properties, including cohesive energy, lattice thermal conductivity and melting temperature. The prediction accuracy is closed to 1 kcal mol^{-1} (0.043 eV $atom^{-1}$) which represents the success of predictions and descriptors. Raccuglia *et al* [71] performed SVM model successfully finding the conditions for the formation of inorganic-organic hybrid materials. The input data which come from the historical reactions were trained to acquire the chemical hypotheses and recommended reactions. While machine learning problems are generally divided into regression problems and classification problems, the mentioned common methods are suitable for both types of problems. In many works, more than one method will be applied simultaneously to get better results.

The advance in the application of machine learning to theoretical calculations is machine learning potentials. Interatomic potentials determine the computational accuracy of molecular dynamics and more accurate interatomic potentials contribute to the broader applications of molecular dynamics. Thus, machine learning potentials have been extensively investigated recently and achieved some success [72–75]. There is an increasing number of valuable articles [76–80] reviewing the application of machine learning potentials. Unke *et al* [81] systematically reviewed the development of machine learning potentials and completely described the physical basis of machine learning potentials. Furthermore, the training process of the machine learning potentials was also described in specific detail. A simplified flow chart can be seen in figure 1.

In this review, the latest studies of machine learning in theoretical computing and practical applications will be overviewed, including machine learning potentials, prediction of thermal and mechanical properties, and materials discovery. The article is organized as below. In section 2, several commonly used machine learning methods are firstly described, including ANN, SVM, and GPR. In section 3, one of the most important progressions of theoretical calculations, machine learning potentials are reviewed. And in section 4, the applications of machine learning to thermal and mechanical properties prediction, and materials discovery will be reported. Finally, the conclusion and challenges of machine learning applications are given in section 5.

Machine learning approaches

Artificial neural network

The artificial neural network is one of the most important methods in machine learning. The simple ANN model contains three layers: an input layer, a hidden layer, and an output layer. Each layer contains a variable number of neurons. The input of the next layer is obtained by linear summation of the weights, the output of the previous layer and the bias. Then the output is obtained by the activation

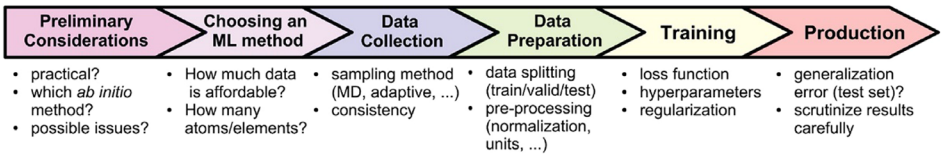

Figure 1. The complete training process of machine learning. Reprinted with permission from [81]. Copyright (2021) American Chemical Society.

function. The above process can be expressed as the following equation:

$$x_{i+1} = h\left(\sum_{i=1}^{n} w_i x_i + b\right), \tag{1}$$

where x_i and x_{i+1} are the output of this layer and next layer, respectively. w_i and b are the weight and bias parameters, respectively and h is the activation function which can be sigmoid function, exponential linear unit (ELU), and rectified linear unit (ReLU). As part of the nonlinear transformation of a neural network, there are certain requirements for the selection of the activation function. The sigmoid function can generally be applied to the left-back layer of the network due to its disadvantage that the gradient of the weights will be close to zero if the input value is large, which can lead to a state where the parameters are updated very slowly or even not updated in deep neural networks. In addition, RELU is widely used in the hidden layer because there is no gradient vanishing problem and the computation is faster for positive inputs. The backpropagation algorithm is used to update the weights during the training process. The loss function is used to determine the final model which means that a smaller loss function represents a better-trained model. The simple loss function can be expressed as:

$$Loss = \sum_{i=1}^{n} (y_i - \hat{y}_i)^2, \tag{2}$$

where y_i is the target value and $\hat{y}_i$ is the predicted value.

Convolutional neural networks (CNN) are a major advancement in neural networks. CNN has gained success and is widely applied in numerous fields, such as computer vision [82], signal processing [83], agriculture [84], etc due to the better learning ability and higher classification accuracy in terms of total complexity. It overcomes the shortcoming of fully connected neural networks that the neglect of the spatial structure and the increasing complexity due to a large amount of input data. The major difference between convolutional neural networks and fully connected neural networks is that the features of the image can be extracted by convolutional and pooling layers. A typical structure of CNN [85] is shown in figure 2, which consists of the convolutional layer, the pooling layer and the fully connected layer. In the convolutional layer, the kernel is the key point that determines the captured features. The purpose of using the pooling layer is to reduce the number of parameters and thus, further reducing the computational complexity. CNN is very useful for object recognition. If the neural networks are well trained and tested, features of images can be recognized automatically, which is a powerful tool in materials classification [86, 87] and identification in different phases [88].

Support vector machines

In general, support vector machines [89] are used in classification and regression problems. Support vector machines are still essentially an optimization problem, i.e. how to optimally partition a data set with the hyperplanes. For example,

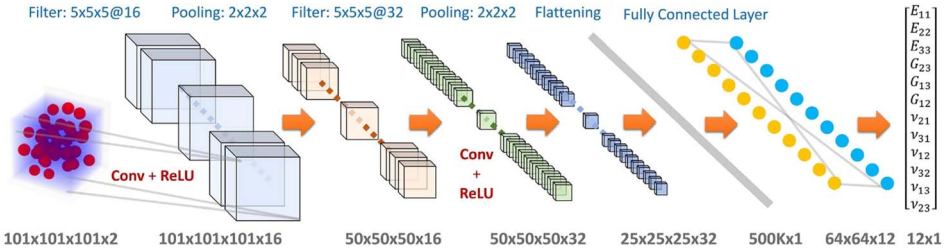

Figure 2. The architecture of CNN which used in properties prediction. It concludes two convolutional layers, two pooling layers and a fully connected layer. Reprinted from [85],© 2020 Elsevier B.V. All rights reserved.

suppose there is a data set (x_i, y_i), the basic equations of SVM are as follow:

$$f(x) = w\varphi(\xi) + b, \tag{3}$$

$$R_{SVMs}(C) = \frac{1}{2}\|w^2\| + C\frac{1}{n}\sum_{i=1}^{n} L(x_i, y_i), \tag{4}$$

where $\varphi(\xi)$ is the high-dimensional space feature. $f(x)$ is the model of hyperplanes that partition the data set and w and b are the weight parameters. R is the objective function, and the optimal partitioning hyperplane can be found by finding its minimum value. However, some samples always cannot be perfectly partitioned, which requires the model to be tolerant of some mistakes that do not satisfy the constraint. The term $C\frac{1}{n}\sum_{i=1}^{n} L(x_i, y_i)$ is introduced to measure this error. C is the error penalty factor and a constant, which is used to reconcile the difference between the regularization term and the empirical error. L represents the loss function. For the optimization problem, in addition to the above objective function, the constraint function needs to come down

$$\begin{aligned} y_i - w\varphi(\xi_i) - b_i &\leqslant \varepsilon + \zeta_i, \\ w\varphi(\xi_i) + b_i - y_i &\leqslant \varepsilon + \zeta_i^*, \\ \zeta_i, \zeta_i^* &\geqslant 0, \end{aligned} \tag{5}$$

where $\zeta_i{}^*$ and $\zeta_i{}^*$ are the slack variables. The above equation can be solved by Lagrange multiplication to obtain its pairing problem.

$$f(x, a_i, a_i^*) = \sum_{i=1}^{n}(a_i - a_i^*)K(x, x_i) + b \tag{6}$$

K is the kernel function that has four types, including linear, sigmoid, polynomial and radial basis functions.

Gaussian process regression

Gaussian process regression is another important machine learning approach for making predictions about materials properties. For a set of input $\{(x_i, y_i) \mid i = 1, 2, \ldots, N\}$, the Gaussian process can be written as:

$$f \sim GP(m, k), \tag{7}$$

where m is the mean function and k is the covariance function. GP stands for the Gaussian process and represents the joint Gaussian distribution. The mean function and the covariance function are expressed as:

$$m(x) = E[f(x)], \tag{8}$$

$$k(x, x') = E[(f(x) - m(x))(f(x') - m(x'))], \tag{9}$$

where E represents the mathematical expectation. This means that if the mean function and covariance function are specified, the Gaussian process is also

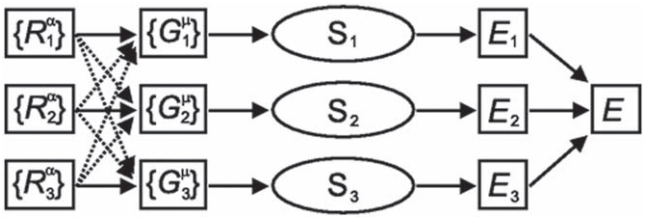

Figure 3. The initial simple structure of the neural network to acquire the NNP. Only three atoms are considered. Reprinted figure with permission from [102], Copyright (2007) by the American Physical Society.

determined. There are many different covariance functions, like squared exponential, matern multiplying $5/2$, exponential, and rational quadratic, etc. A common example of mean function and covariance function is as follow:

$$m(x) = ax + b, \tag{10}$$

$$k(x, x') = \mathrm{cov}(f(x), f(x')) = \sigma_f^2 \exp\left(-\frac{\|x - x'\|^2}{2l^2}\right), \tag{11}$$

where σ_f^2 and l are the hyperparameters of the kernel function. In fact, in GPR, the function $f(x)$ is not accessible in most applications. Thus, $f(x)$ is denoted as:

$$y_i = f(x_i) + \varepsilon_i, \tag{12}$$

where ε is an i.i.d. noise variable that obeys $N(0,\sigma^2)$ where $\sigma^2$is the variance.

Theoretical applications of machine learning

Machine learning potential is one of the major breakthroughs in the application of machine learning to computing. Interatomic forces between atoms in molecular dynamics are typically described with empirical interatomic potentials (EIPs). A large number of different forms of EIPs functions, like Tersoff [90–92], REBO [93], EAM [94], reactive force field [95–97] (ReaxFF), etc, have been developed and applied to different systems by molecular dynamics simulations with some success. Whereas this accuracy is limited due to the pre-defined mathematic formulation. In addition, although the parameters of EIPs can be optimized [98], the optimization problem remains a challenge [99], especially for the complex EIPs, like ReaxFF [100].

Machine learning provides a new way to acquire the relationships between atomic configurations and energy. Several machine learning potentials have been proposed in recent years based on the different machine learning models and descriptors, such as neural networks potentials [101, 102] (NNP), Gaussian approximation potentials [103] (GAP) and moment tensor potential [104] (MTP). In addition, machine learning potential packages, like Deep-MD [105] and QUIP [106], have been developed and integrated into common molecular dynamics simulation software, such as LAMMPS [107], etc. In this section, three common machine learning potentials are introduced, including NNP, GAP and MTP.

Neural networks potentials

The original study of NNP came from the work of Behler *et al* [102]. As shown in figure 3, the coordinates of each atom are used as inputs. Then, those inputs are converted into a serial of symmetry function values. Afterward, the neural network is used to obtain the predicted energy values. It is worth noting that the total energy of the system is the sum of energies of each atom. The energy of each atom is determined by its chemical environment which is described by physical descriptors. In this work, the descriptors are called symmetry functions. The

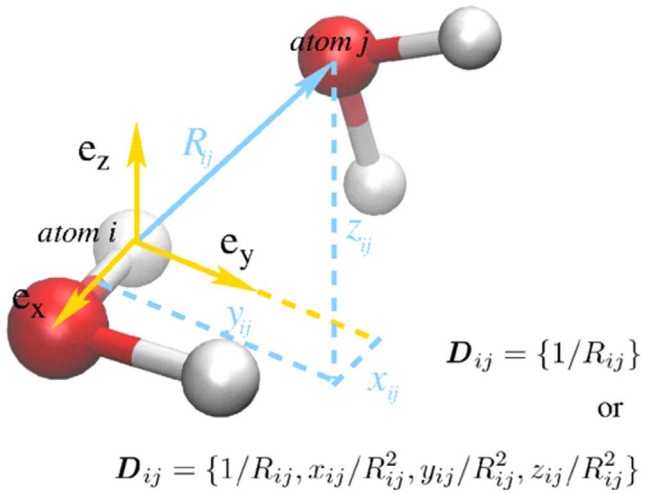

Figure 4. To illustrate this with the example of a water molecule, the input to the neural network represents the environment of atom *i*. Reprinted figure with permission from [101], Copyright (2018) by the American Physical Society.

symmetry function consists of two parts, the radial term and the angular term, denoted as:

$$G^1 = \sum e^{-\eta(R_{ij}-R_s)^2} f_{cut}(R_{ij}), \tag{13}$$

$$G^2 = 2^{1-\varsigma} \sum (1 + \lambda \cos\theta_{ijk})^{\varsigma} \times e^{-\eta(R_{ij}^2+R_{ik}^2+R_{jk}^2)} f_c(R_{ij}) f_c(R_{ik}) f_c(R_{jk}), \tag{14}$$

where G^1 and G^2 are the radial term and angular term, respectively. R_s, η and ζ are the parameters that are selected by experience. Different values of R_s, η and ζ have been used resulting in a few thousand fitting parameters for the NN. R_{ij} is the distance between atom i and j. θ_{ijk} is the angle of atom i, j and k, and the center is the atom i. f is the cutoff function which can be expressed as:

$$f_c(R_{ij}) = \begin{cases} 0.5[\cos(\pi R_{ij}/R_c) + 1] & R_{ij} \leqslant R_c \\ 0 & R_{ij} > R_c \end{cases}. \tag{15}$$

This equation implies that if the atom distance exceeds the cutoff distance, there is no interaction between two atoms. And it ensures that the energy varies smoothly with distance.

Although the development of this potential function is best applied to the single-element system, this work is very enlightening. And next, different ANNs were developed and one common example is deep potential molecular dynamics [101, 105] (DPMD). DPMD is the scheme for molecular dynamics simulations that used neural network potentials. It is also an NNP but its breakthrough lies in overcoming the limitations of symmetry functions. The calculated four quantities $1/R_{ij}$, x_{ij}/R_{ij}, y_{ij}/R_{ij} and z_{ij}/R_{ij} are only the input of the deep neural networks. A specific image example can be seen in figure 4. And next, the input quantities are transformed into descriptors by embedding net. Another difference is that DPMD is based on the deep neural network which contains multiple hidden layers. The proposed DPMD is proven to be effective and feasible in multiple systems [108–111].

Fan *et al* [112] proposed a novel neural network potential that incorporates an evolutionary strategy, called the neuroevolutionary potential (NEP). A new descriptor was developed which was inspired by the symmetry functions and the smooth overlap of atomic positions (SOAP). As an example of single-component

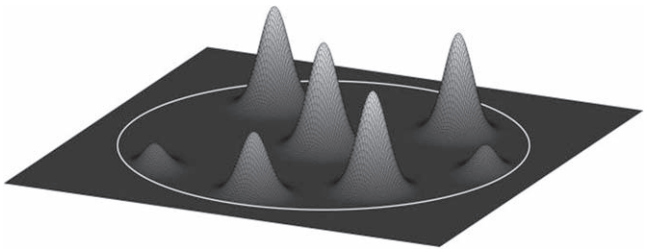

Figure 5. The illustration of the atomic neighborhood density function. [106] John Wiley & Sons. © 2015 Wiley Periodicals, Inc.

systems, the radial term and angular term are expressed as:

$$q_n = \sum g_n(r_{ij}), \tag{16}$$

$$q_{nl} = \sum\sum g_n(r_{ij}) g_n(r_{ik}) P_l(\cos\theta_{ijk}). \tag{17}$$

A detailed description of these two functions can be found in the article by Fan *et al* [112]. Importantly, this potential was integrated into the molecular dynamics software that uses GPU calculations which are called GPU-MD [113, 114] and this potential is reported to be faster than some other machine learning potentials, such as GAP and DP.

Gaussian approximation potentials

Some of the physical assumptions of Gaussian approximation potentials are the same as for the neural network potentials. The system energy can be described as the sum of the energies of each atom and the energy of the atom is determined by its surroundings. In GAP, the atomic energy is the sum of a series of kernel functions associated with the descriptor:

$$E(q_i) = \sum_{t=1}^{N_t} \alpha_t \, K(q_i, q_t), \tag{18}$$

where E, K, and q are the atomic energy, the kernel function, and the descriptor, respectively. For the two-body descriptors, q is described as:

$$q^2 = |r_i - r_j|. \tag{19}$$

For the three-body term, the equation is

$$q^3 = \begin{Bmatrix} r_{ij} + r_{ik} \\ (r_{ij} - r_{ik})^2 \\ r_{jk} \end{Bmatrix}. \tag{20}$$

The many-body term is usually represented by SOAP. The SOAP kernel can be written as:

$$K(\rho, \rho') = \int dR \left| \int \rho(r)\rho(Rr)dr \right|'', \tag{21}$$

where ρ is the Gaussian function represented the local density [115].

$$\rho(r) = \sum \exp\left(-\frac{(x_i - r)^2}{2\sigma^2} \right). \tag{22}$$

The detailed description of SOAP can be found in De *et al* [115] and a two-dimensional diagram of local density function is illustrated in figure 5. An example of the use of GAP was shown in the work of Rowe *et al* [116]. Gaussian approximation potential for graphene was trained with computational data from the density functional theory (DFT). Also, to access the accuracy of the machine learning potentials, phonon dispersion curves and phonon spectra at finite

temperature were calculated and compare to the results from DFTB and the empirical interaction potentials, including REBO, AIREBO, AIREBO-Morse, Tersoff and ReaxFF. The phonon spectrum calculated by GAP are consistent with the experimental results and the sub-meV accuracy can reach.

Moment tensor potential

As with the two machine learning potentials above, the total energy in moment tensor potential can be attributed to the contribution of each atom, while also using the concepts of neighboring atoms and cutoff. The atomic contribution is denoted as:

$$V(r_i) = \sum \theta_j B_j(r_i), \tag{23}$$

where B is the basis function and θ is the parameter that needs to be calculated by fitting to the training set. Energy, force, and stress tensor are used to determine the final MTP. The parameters in MTP are optimized by a minimization function.

$$\sum \left[C_E^2 \Delta E(x_i)^2 + C_f^2 \sum \Delta f_j(x_i)^2 + C_s^2 \Delta \sigma(x_i)^2 \right], \tag{24}$$

where ΔE, Δf and $\Delta \sigma$ are the errors of energy, force and stress, respectively, which is the difference between the prediction value and the target value. And C_E, C_f and C_s are the weighting parameters. A detailed description of MTP can be seen in the work of Shapeev *et al* [104]. Discrepancy representations of the atomic environment can be also found in this work which is based on the invariant polynomials.

Applications of AI in engineering

Thermal property

Thermal transportation has gained increasing attention due to its important role in high-power density electronic devices [117–119], thermal materials [120–123], thermoelectric materials [124, 125] and aerospace [126, 127]. In particular, in micro and nanoscale areas, some peculiar phenomena different from the traditional understanding were discovered, like size effects [128, 129] and thermal rectification [130, 131]. In addition, one-dimensional and two-dimensional materials, such as carbon nanotube [132–134] and graphene [135–140], provide additional opportunities to investigate the theoretical microphysical phenomena. Thermal conductivity and thermal resistance are the common but essential materials properties. As mentioned above, experimental measurements and theoretical calculations of the thermal properties of materials have been important efforts. Machine learning provides a new way to make a reasonable prediction of thermal conductivity and thermal resistance. There are two ways to predict the thermal properties of materials, one based on the machine learning models and the other on molecular dynamics driven by machine learning potentials. In the following part of this section, the works on thermal properties prediction based on the above two methods are reported.

The machine learning models used in thermal properties prediction are not uniform. Several machine learning models are used, such as fully connected neural networks, CNN, SVM, GPR, etc. Han *et al* [141] utilized a genetic algorithm-driven approach and machine learning methods to investigate the effect of porous structure on the thermal conductivity of materials. The conventional view of physics holds that periodically distributed porous structure has a higher thermal conductivity compared to disordered porous structure [142–144]. This view is challenged in this work. By using the genetic algorithm-driven approach, the

unexpected enhanced thermal conductivity in disordered nanoporous graphene is discovered. To further investigate this unexpected finding, a series of descriptors affecting the thermal conductivity of nanoporous materials were proposed, including shape factor, bottleneck, channel factor, perpendicular nonuniformity, and dominant paths. Regression analysis revealed the correlation between these descriptors and the thermal conductivity of nanoporous materials (see figure 6). It is found that more pore arrangement in the *x*-direction improves thermal conductivity, while more pore arrangement in the *y*-direction leads to a decrease in thermal conductivity. In addition, machine learning approaches were also used to predict the thermal conductivity of nanoporous graphene, and the predictions were reasonable and accurate [145]. Machine learning methods have been shown to not only make predictions about thermal conductivity but also to help find new physical insights. Chen *et al* [146] used GPR to predict the thermal conductivity of inorganic materials and the data for the training set is derived from the experiments. They summarized 29 features to investigate the relevance of thermal conductivity, including bulk modulus, density, mean average bond length, etc. Next, by using the summarized features and machine learning model, 95 sets of data are utilized to train the model and make credible predictions of 5 inorganic solids in the hold-out set. Also, a comparison of this training model and other semi-empirical models is taken. The ML model presented in this work is cheaper and more flexible contributing to the easily and fast accessible chemical and structural features. The prediction of thermal resistance is a challenging task because of the variety of factors that determine the interface thermal resistance. Wu *et al* [147] employed three different machine learning models, including regression tree ensembles of LSBoost, SVM, and GPR, to predict the interfacial thermal resistance, with the data from experiments. The predicted results were illustrated in figure 7(b) and the differences in the predictions of the three models can be seen in figure 7(a). The effects of descriptors were also considered. These descriptors were categorized into three types, including property descriptors, compound descriptors, and process descriptors (see in figure 7(c)). As the number and type of descriptors provided increase, this means that more information is considered, and the accuracy of the prediction model increases. In addition, it also means that the influence of descriptors in thermal resistance cannot be considered in isolation.

Machine learning potential-driven molecular dynamics is another approach to predict the thermal properties which provide additional physical insights. Liu *et al* [148] developed the MTP for Wurtzite Boron Arsenide to investigate the influence of four-phonon scattering in thermal conductivity. Boltzmann transport equation is a common method to calculate the lattice thermal conductivity, but the requirement of the higher-order interatomic force constants (IFC) is the challenge. The computational speed and efficiency of high order IFC calculation with density functional theory and machine learning potentials were directly compared. It was found that the computational effort to obtain higher-order IFC using MTP was greatly reduced. Meanwhile, the thermal conductivity of Wurtzite Boron Arsenide is 1036 W m^{-1} K^{-1} which decreased by 43% considering the four-phonon scattering (see figure 8). Hiphive package [149] provides another effective method to extract high-order IFC from a limited amount of data set. In this package, the symmetry of crystal was considered to reduce the number of degrees and machine learning methods was used to extract arbitrary order IFC based on the data set acquired from DFT. In addition, the absence of a reliable force field is one of the biggest obstacles in molecular dynamic simulations. Machine learning potentials remove this barrier. Liu *et al* [150] developed the GAP for β-Ga_2O_3 to study the thermal properties overcoming the limitation of the lack of force field for β-Ga_2O_3. By using *ab initio* molecular dynamics and static calculations, 800 sets of data, including configurations, total energies, forces, and virial stresses were obtained

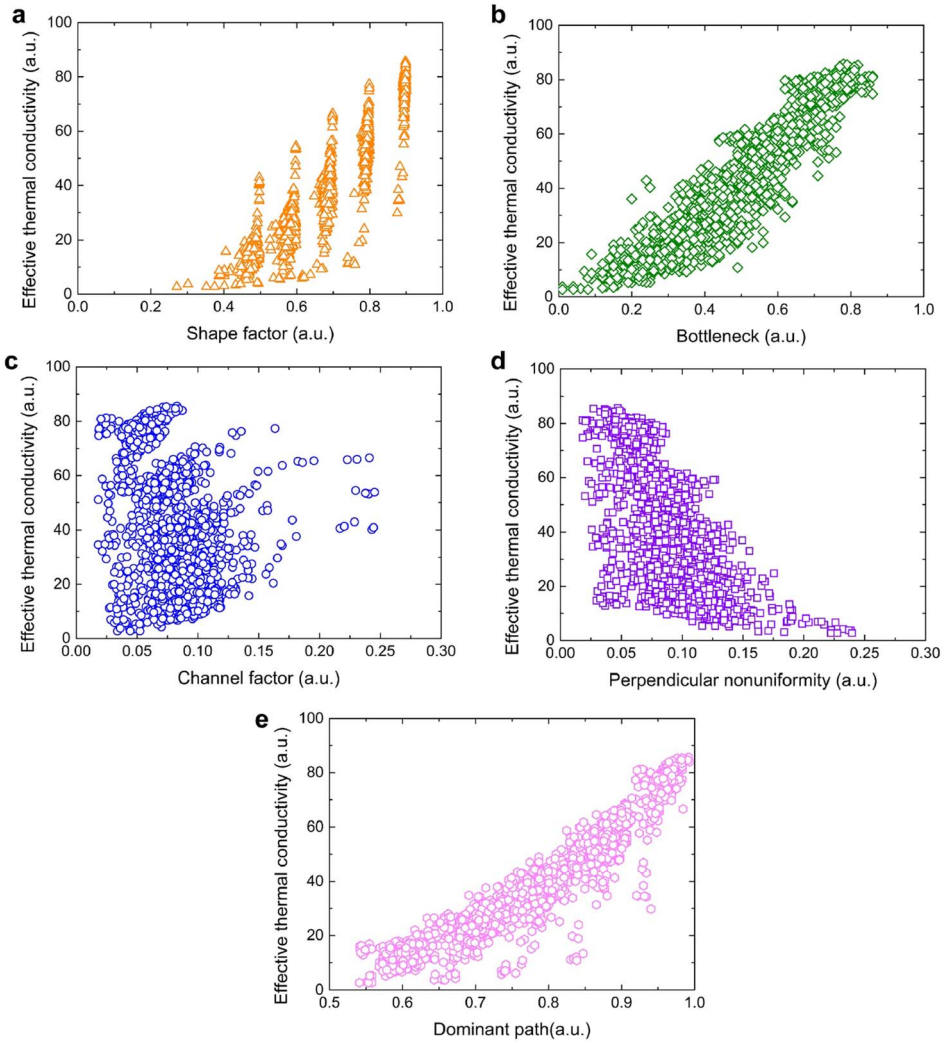

Figure 6. The correlation between effective thermal conductivity and five different physical descriptors (a) shape factor, (b) bottleneck, (c) channel factor, (d) perpendicular nonuniformity, (e) dominant path. Reprinted from [145], © 2020 Elsevier Ltd. All rights reserved.

and used to train the GAP. This trained GAP can reach high accuracy, 0.0003 eV atom^{-1} for energy accuracy, 0.050 eV Å and 0.038 eV Å^{-1} for different atomic force accuracy. Subsequently, the large-scale atomic system simulations were performed to verify the capacity of this trained GAP in predicting the lattice dynamics, the thermal conductivity of β-Ga_2O_3 and the interlayer interactions between β-Ga_2O_3 and substrate. Li *et al* [151] also predicted the thermal conductivity of β-Ga_2O_3 but the interatomic interaction potential was deep NNP. The predicted values were consistent with the calculated value from the first principles. In addition, the anisotropic thermal conductivity of β-Ga_2O_3 was found, 10.68 W m^{-1} K^{-1} in the [110] direction, 20.78 W m^{-1} K^{-1} in the [010] direction, and 12.61 W m^{-1} K^{-1} in the [001] direction. These all support the great potential of machine learning potential in predicting the thermal properties of materials.

Mechanical property

Mechanical properties are another common but important physical property. Materials applied in devices inevitably confront the deformation [152, 153], shear, etc. Therefore, measuring and calculating the mechanical properties is one of the essential parts of the studies of material properties. Like thermal properties,

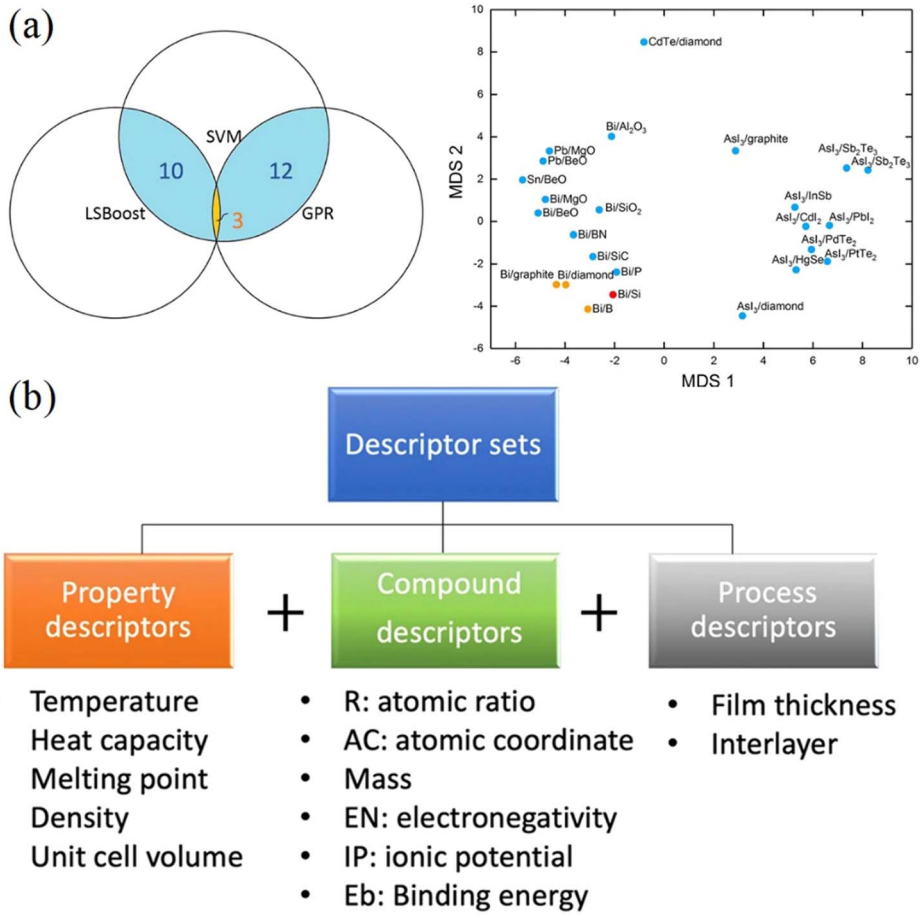

Figure 7. (a) Interface thermal resistance of different systems were predicted by three machine learning models, including SVM, GPR and LSBoost. The color region represents the interface thermal resistance were predicted repeatedly by at least two models. (b) The list of descriptors. Reproduced from [147]. CC BY 4.0.

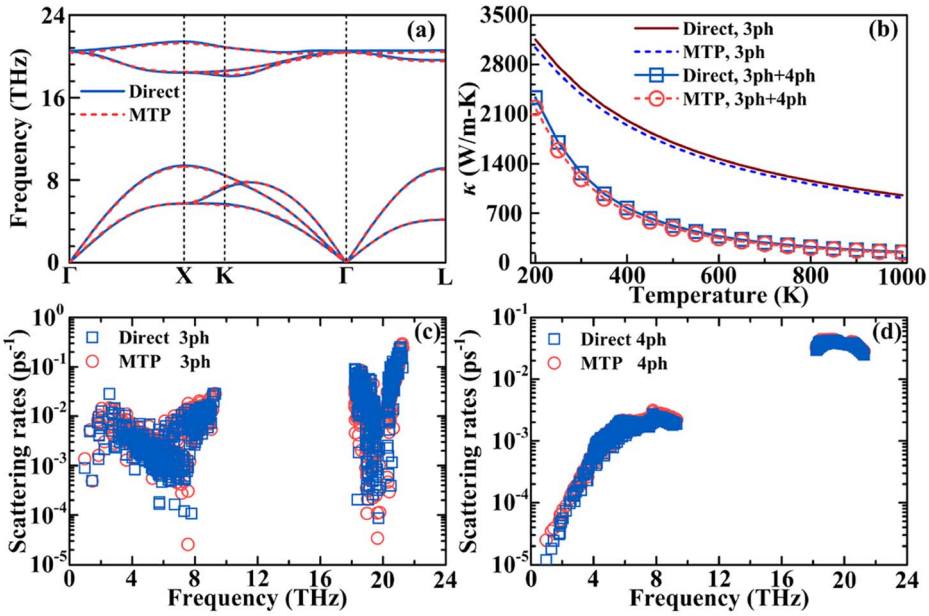

Figure 8. (a) Phonon spectrum of c-Bas with direct calculations and MTP. (b) Thermal conductivity with Three-phonon and four-phonon scattering considerations. (c)–(d) Comparison of three-phonon and four-phonon scattering pairs for scattering rate variation with frequency. Reprinted with permission from [148]. Copyright (2021) American Chemical Society.

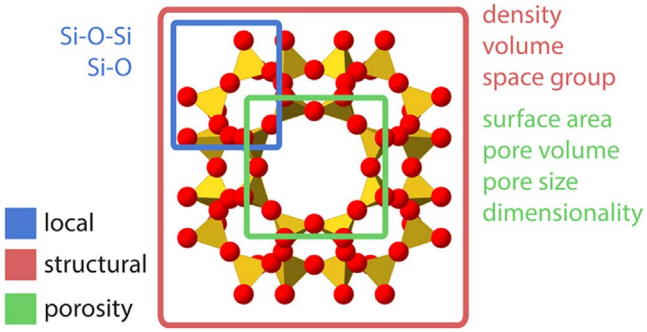

Figure 9. A classification of descriptors which used in mechanical properties prediction of zeolite frameworks. Reprinted with permission from [160]. Copyright (2017) American Chemical Society.

mechanical properties study can be divided into two parts, including experimental measuring and theoretical calculations. In recent years, machine learning methods are also expanded to the field of mechanical properties prediction. Zeolites are widely used for adsorption [154, 155], separation [156, 157], and gas storage [158, 159] due to their nanoporous structures. However, the unique and rich structures also give rise to variations in properties. Mechanical properties are one of the key factors to determine the viable zeolite's structure. And this structure diversity makes the determination more challenging and expensive. A simpler and cheaper properties prediction method is needed. By using gradient boosting regressor, Evans *et al* [160] predicted the moduli for 590448 hypothetical zeolites. The trained data, including bulk and shear moduli, were derived from exact DFT calculations. This is an unacceptably expensive undertaking if traditional measurement and calculation methods are used. But using machine learning methods, it is cheaper and less time-consuming. In this study, about 32 descriptors were acquired from the geometric information (see figure 9), such as internal surface area, pore-volume, features of the distribution of bond lengths and angles, etc. Excellent accuracy was achieved with a root mean square error of 0.102 and 0.0847. For other materials, such as silica with various crystal structures and glassy states, graphene, etc, machine learning methods have also shown excellent mechanical property prediction capabilities. Deng *et al* [161] explored the relationship between mechanical properties and complex structural properties of silica by using machine learning methods and enhanced sample methods. The descriptors of various types of silica were acquired from DNN (see in figure 10(a)) and the results showed that the DNN method provided the precise prediction of mechanical properties of silicon dioxide (see in figure 10(b)). Zhang *et al* [162] employed several different machine learning models, like stochastic gradient descent, k-nearest neighbors, support vector machine, decision tree, and artificial neural networks, to investigate the mechanical properties of graphene. And it was found that stochastic gradient descent method was not suitable for the predictions of mechanical properties in this study. The training data sets were derived from the molecular dynamics calculations and the influence factors, temperature, strain rate, vacancy defect, and chirality, were considered. Integrating the effects of multiple factors is difficult using traditional methods, but it is achievable for machine learning methods.

Moreover, by using the machine learning potentials, computational accuracy of mechanical properties of materials can reach near the level of DFT while allowing for large-scale calculations. Mortazavi *et al* [163] investigated the mechanical properties of graphene/borophene heterostructures by employing MTP. For empirical interatomic potential, the calculations of mechanical properties of graphene/borophene heterostructures are inaccurate and unstable. However, by using the machine learning potential, the calculated ultimate tensile strengths of the graphene/borane heterostructure agree well with the DFT

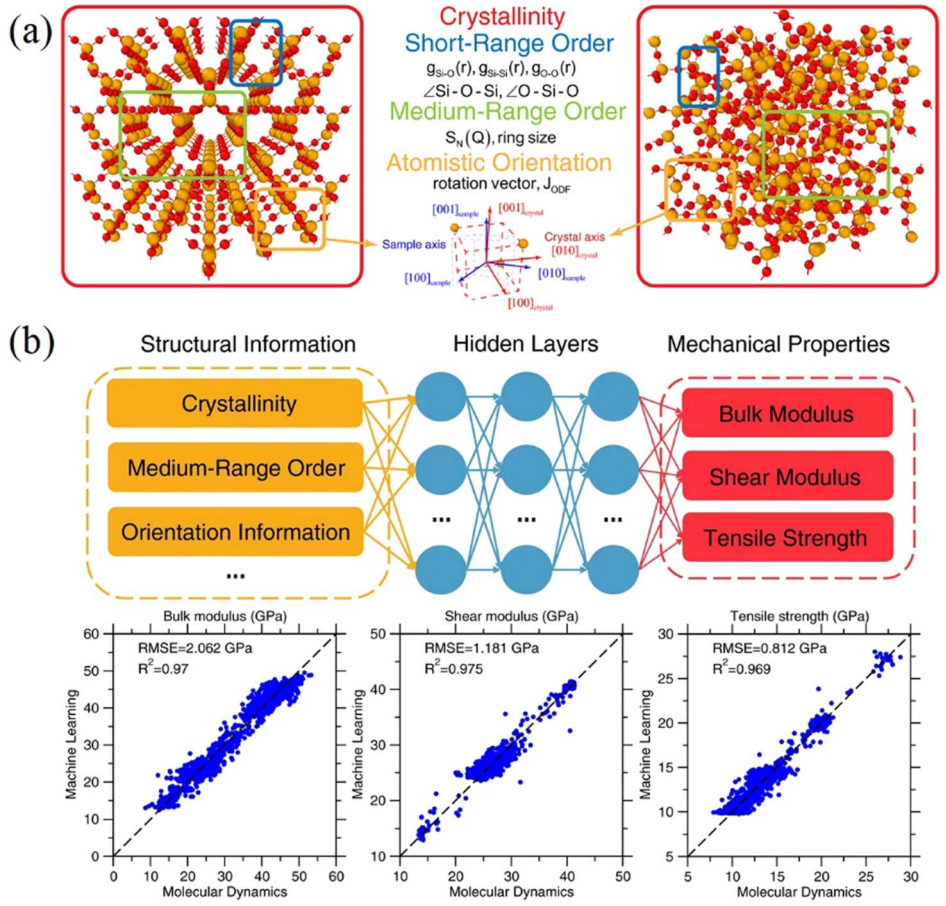

Figure 10. (a) Vivid illustrated of the descriptors which used in the mechanical properties prediction by machine learning methods. (b) The prediction model and error of bulk modulus, shear modulus and tensile strength. [161] John Wiley & Sons.© 2021 The American Ceramic Society.

calculations. Although there are still discrepancies for some structures, this is a great improvement over the empirical potential. Moreover, multi-scale modeling is also possible through the utilization of machine learning potentials (see figure 11). Graphene/borane heterostructure models with sizes ranging from 63 nm to 63 μm were constructed, and the deformation process was observed. These highlight the capacity of machine learning potentials in multi-scale calculations and the predictions of complex system properties.

Computational material discovery

Materials play a fundamental role in modern society. The search and discovery of desired materials through assisted machine learning methods [164–167] were widely studied and used in recent years. Thermoelectric materials have been extensively studied due to their unique properties to directly convert waste heat and thermal energy into electrical energy [168–171]. The conversion efficiency of thermoelectric materials depends on the thermoelectric figure of merit ZT, which is defined as:

$$ZT = \frac{\alpha^2 T}{\rho(k_L + k_e)}, \tag{25}$$

where α is the Seebeck coefficient, T is the temperature and ρ is the electrical resistivity. k_L and k_e represent the lattice thermal conductivity and charge-carrier thermal conductivity, respectively. The improvement of thermoelectric efficiency is a daunting challenge because it is determined by numerous factors and

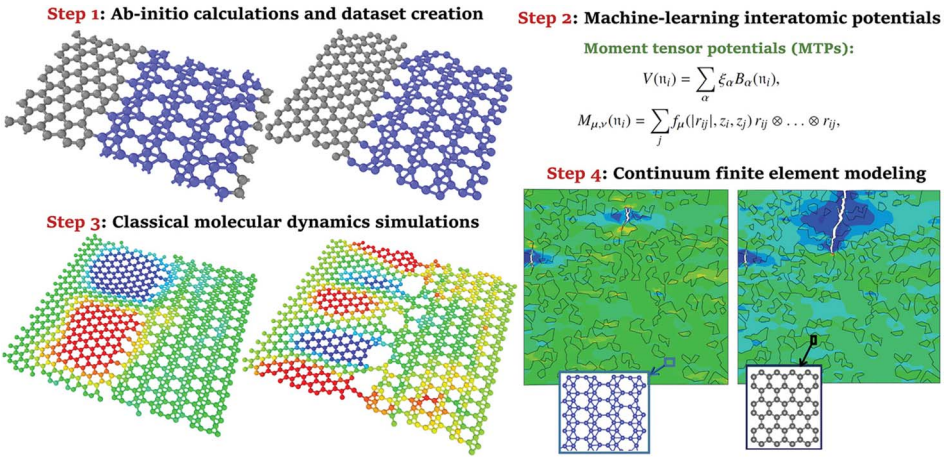

Figure 11. Multi-scale modeling calculations of graphene/borophene heterostructures. Reproduced from [163]. CC BY 4.0.

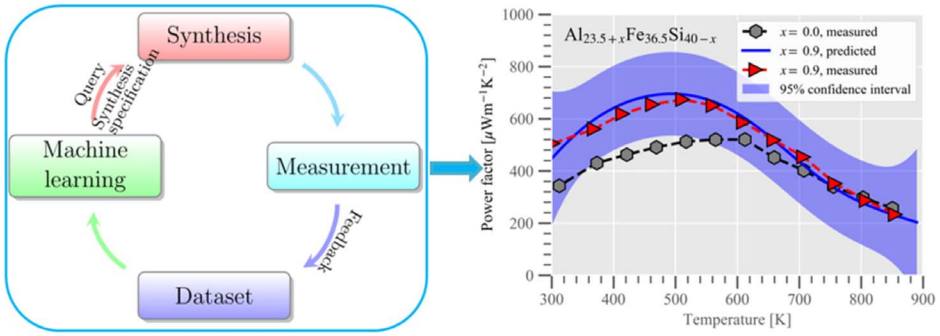

Figure 12. The process and result of using machine learning approach to find the optimized Al/Si ratio. Reprinted with permission from [174]. Copyright (2019) American Chemical Society.

meanwhile, there are complex interrelationships between the factors. For example, electrons and phonons together determine the thermoelectric properties of the material. In addition to some properties that determine electrons and phonons separately, there are interactions between electrons and phonons. These electron-phonon interactions influence the thermal conductivity and Seebeck coefficient [172].

In the past research on thermoelectric materials, theoretical calculations, especially DFT calculations, have made a great contribution [170, 173]. Thermoelectric material discovery aided by machine learning algorithms has become popular, recently. Hou *et al* [174] utilized the GPR model to find the optimized power factor of $Al_2Fe_3Si_3$ intermetallic compound (see figure 12). This intermetallic compound has been reported to have a high-power factor in the middle-temperature range. $Al_{23.5+x}Fe_{36.5}Si_{40-x}$ can reach the higher power factor by optimizing the ratio x. The training data sets, including temperature, compound, and power factor, were acquired from experiment measurement. Next, the relationships of temperature, compound and power factor were obtained by the GPR model and according to this model, power factor with different temperature and compound was predicted for finding the optimized power factor. The final optimized ratio x was found to be 0.9. It is worth noting that the cost and time to discover the optimal ratio by using a machine learning model is minimal compared to the experiment. Iwasaki *et al* [175] employed a serial of machine learning methods, including decision tree regression, elastic net, quadratic polynomial LASSO, and neural network to investigate the key parameters controlling the spin-driven thermoelectric effect. The model schematic is shown in figure 13(a). Next,

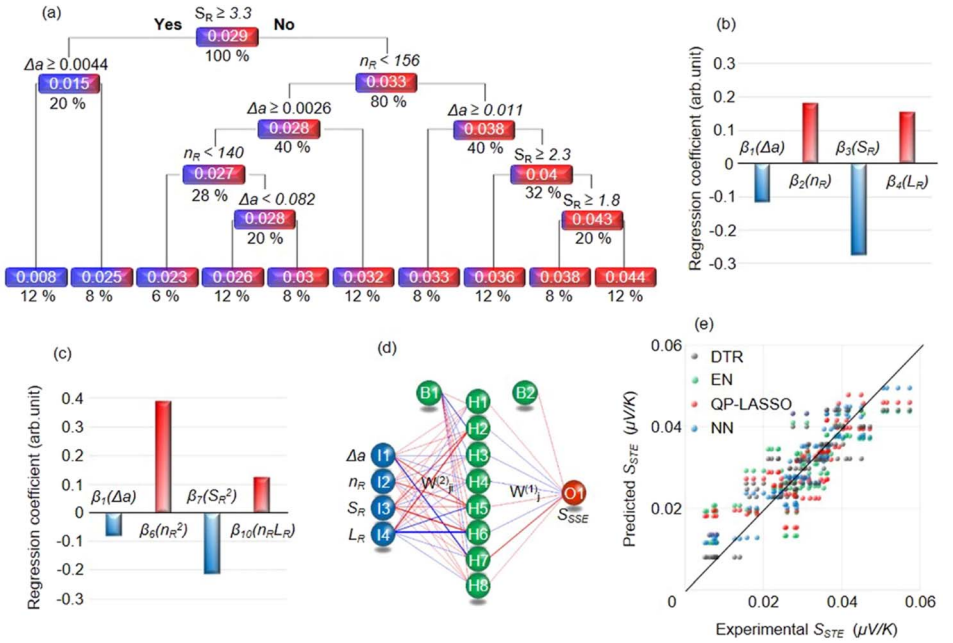

Figure 13. (a) A schematic diagram of decision tree regression while $\Delta\alpha$ and S_R have positive correlation and n_R has a negative correlation with spin-driven thermoelectric effect. (b)–(c) Regression coefficients for the elastic net and quadratic polynomial LASSO. (d) A schematic diagram of neural network. (e) Comparison graph of predicted and experimental results. Reproduced from [175]. CC BY 4.0.

these trained models helped to develop new spin-driven thermoelectric effect materials. In this study, Fe-Pt-Sm alloy has been selected and optimized which demonstrated the feasibility of this model.

However, the 'global optima' for thermoelectric materials discovery remains an intractable problem. Most of the works are limited only to locally optimal solutions even using machine learning methods. Gaultois *et al* [176] offered a different insight. A machine learning-based engine for materials recommendation was developed to provide the potentially viable material selection options rather than the quantitative predictions of properties.

Conclusion and future challenges

This review focuses on the theoretical and practical applications of ML in computational nanotechnology, including machine learning potentials, thermal properties, and mechanical properties prediction and materials discovery. The most common machine learning methods are first presented, followed by a systematic report of significant advances in machine learning potentials, such as NNP, GAP and MTP. In addition, those machine learning potentials have been integrated into the software, like GPUMD, QUIP, etc. The application of machine learning in thermal and mechanical properties prediction was highlighted in two parts, including the utilization of machine learning models and molecular dynamics simulations driven by machine learning potentials. Machine learning models make the reasonable prediction of material properties and machine learning potential combines the advantages of DFT and empirical potential in a computationally promising way.

However, there are remaining challenges with the application of machine learning. (1) The number of reliable training sets is often insufficient to meet the number of training sets required for machine learning training. It is a great challenge to train the model with a small training set to obtain predictions with

acceptable accuracy. Moreover, the data from successful experiments are far more than failed experimental data and these data also have some value and significance [71]. (2) Descriptors are crucial for the properties prediction using machine learning methods. Although as mentioned above, more information consideration will improve the performance of machine learning models, the increasing number of descriptors increases the complexity of the calculation. For high-dimensional problems, there is a need to develop more efficient and concise descriptors. (3) For machine learning potentials, the problems of data sets and descriptors are also possessed, especially for materials with complex chemical compositions. The need for a large amount of data sets and increasing descriptors lead to the fact that the training of machine learning potentials is extremely difficult, complex, time-consuming, and costly.

Acknowledgments

YY acknowledges the financial support from the National Key Research and Development Program of China (no. 2019YFE0119900), National Natural Science Foundation of China (no. 52076156). JZ thanks for the support of this work from NVIDIA AI Technology Center (NVAITC). The authors appreciate the support from the Supercomputing Center of Wuhan University.

Data availability statement

No new data were created or analysed in this study.

Conflict of interest

Authors have no conflict of interest to declare.

ORCID iDs

Zhongtao Zhang https://orcid.org/0000-0002-1304-1691
Yanan Yue https://orcid.org/0000-0002-3489-3949
Jingchao Zhang https://orcid.org/0000-0001-5289-6062

References

[1] Arslan E, Schulz J and Rai K 2021 Machine learning in epigenomics: insights into cancer biology and medicine *Bba.-Rev. Cancer* **1876** 188588
[2] Antoniou T and Mamdani M 2021 Evaluation of machine learning solutions in medicine *Can. Med. Assoc. J.* **193** E1425–9
[3] Elbadawi M, McCoubrey L E, Gavins F K H, Ong J J, Goyanes A, Gaisford S and Basit A W 2021 Disrupting 3D printing of medicines with machine learning *Trends Pharmacol. Sci.* **42** 745–57
[4] Henarejos-Castillo I *et al* 2021 Machine learning-based approach highlights the use of a genomic variant profile for precision medicine in ovarian failure *J. Pers. Med.* **11** 609
[5] Infante T, Francone M, De Rimini M L, Cavaliere C, Canonico R, Catalano C and Napoli C 2021 Machine learning and network medicine: a novel approach for precision medicine and personalized therapy in cardiomyopathies *J. Cardiovasc. Med.* **22** 429–40
[6] Artrith N, Butler K T, Coudert F X, Han S, Isayev O, Jain A and Walsh A 2021 Best practices in machine learning for chemistry comment *Nat. Chem.* **13** 505–8
[7] Gormley A J and Webb M A 2021 Machine learning in combinatorial polymer chemistry *Nat. Rev. Mater.* **6** 642–4

[8] Ivonina M V, Orimoto Y and Aoki Y 2021 Quantum chemistry-machine learning approach for predicting and elucidating molecular hyperpolarizability: application to [2.2] paracyclophane-containing push-pull polymers *J. Chem. Phys.* **154** 124107

[9] Goh G B, Hodas N O and Vishnu A 2017 Deep learning for computational chemistry *Journal of Computational Chemistry* **38** 1291–307

[10] Maestrales S, Zhai X M, Touitou I, Baker Q, Schneider B and Krajcik J 2021 Using machine learning to score multi-dimensional assessments of chemistry and physics *J. Sci. Educ. Technol.* **30** 239–54

[11] Prezhdo O V 2020 Advancing physical chemistry with machine learning *J. Phys. Chem. Lett.* **11** 9656–8

[12] Shaughnessy A R, Gu X, Wen T and Brantley S L 2021 Machine learning deciphers CO2 sequestration and subsurface flowpaths from stream chemistry *Hydrol. Earth Syst. Sci.* **25** 3397–409

[13] Hong Y, Hou B, Jiang H and Zhang J 2020 Machine learning and artificial neural network accelerated computational discoveries in materials science *WIREs Computational Molecular Science* **10** e1450

[14] Ju C W, Bai H Z, Li B and Liu R Z 2021 Machine learning enables highly accurate predictions of photophysical properties of organic fluorescent materials: emission wavelengths and quantum yields *J. Chem. Inf. Model.* **61** 1053–65

[15] Zhu X Z, Wan Z H, Tsang D C W, He M J, Hou D Y, Su Z S and Shang J 2021 Machine learning for the selection of carbon-based materials for tetracycline and sulfamethoxazole adsorption *Chem. Eng. J.* **406** 126782

[16] Wang X, Wang W, Yang C, Han D, Fan H and Zhang J 2021 Thermal transport in organic semiconductors *J. Appl. Phys.* **130** 170902

[17] Zhang J 2021 Application of artificial intelligence in renewable energy and decarbonization *ES Energy Environ.* **14** 1–2

[18] Ong S P 2019 Accelerating materials science with high-throughput computations and machine learning *Computational Materials Science* **161** 143–50

[19] Hong Y, Han D, Hou B, Wang X and Zhang J 2021 High-throughput computations of cross-plane thermal conductivity in multilayer stanene *Int. J. Heat Mass Transfer* **171** 121073

[20] Goldsmith B R, Esterhuizen J, Liu J X, Bartel C J and Sutton C 2018 Machine learning for heterogeneous catalyst design and discovery (vol 64, pg 2311, 2018) *Aich. J.* **64** 3553

[21] Guo Y *et al* 2021 Machine-learning-guided discovery and optimization of additives in preparing Cu catalysts for CO2 reduction *J. Am. Chem. Soc.* **143** 5755–62

[22] Dasgupta A, Gao Y, Broderick R, Pitman E B and Rajan K 2020 Machine Learning-Aided Identification of Single Atom Alloy Catalysts *The Journal of Physical Chemistry C* **124** 14158–66

[23] Sun M Z, Dougherty A W, Huang B L, Li Y L and Yan C H 2020 Accelerating atomic catalyst discovery by theoretical calculations-machine learning strategy *Adv. Energy Mater.* **10** 1903949

[24] Suzuki K, Toyao T, Maeno Z, Takakusagi S, Shimizu K and Takigawa I 2019 Statistical analysis and discovery of heterogeneous catalysts based on machine learning from diverse published data *ChemCatChem* **11** 4537

[25] Dargar A and Srivastava V M 2021 Performance comparison of stacked dual-metal gate engineered cylindrical surrounding double-gate MOSFET *Int. J. Electron. Telec.* **67** 29–34

[26] DiStefano J G, Murthy A A, Hao S Q, dos Reis R, Wolverton C and Dravid V P 2020 Topology of transition metal dichalcogenides: the case of the core–shell architecture *Nanoscale* **12** 23897–919

[27] Prasad H D R and Sitaram N 2021 Performance of nano materials for the strength development in concrete cube used as Partial replacement for cement at different temperatures *Mater. Today-Proc.* **45** 7253–8

[28] Rangel A E, Hariri A A, Eisenstein M and Soh H T 2020 Engineering aptamer switches for multifunctional stimulus-responsive nanosystems *Adv. Mater.* **32** 2003704

[29] Sharmila D J, Suresh V, Emmanuel B P, Arnold E M, Praveen B, Pugazhendhi K and Shyla J M 2021 Optimization of ZnO doped TiO2 nanopillars as photoanode for dye sensitized solar cells *Mater Today-Proc.* **45** 1166–9

[30] Sinitsin D A, Shayakhmetov U S, Rakhimova O N, Khalikov R M and Nedoseko I V 2021 Nanostructured foam ceramics for building purposes: production technology and applications *Nanotechnol. Construct.* **13** 213–21

[31] Wang C S, Yu Y J, Irfan M, Xu B L, Li J J, Zhang L H, Qin Z H, Yu C Y, Liu H Y and Su X 2020 Rational design of DNA framework-based hybrid nanomaterials for anticancer drug delivery *Small* **16** 2002578

[32] Zhou X W, Jiang X, Qu M Y, Aninwene G E, Jucaud V, Moon J J, Gu Z, Sun W J and Khademhosseini A 2020 Engineering antiviral vaccines *Acs Nano* **14** 12370–89

[33] Zhou X X, Wang Y, Gong c.c., Liu B and Wei G 2020 Production, structural design, functional control, and broad applications of carbon nanofiber-based nanomaterials: a comprehensive review *Chem. Eng. J.* **402** 126189

[34] Zhang J, Huang X, Yue Y, Wang J and Wang X 2011 Dynamic response of graphene to thermal impulse *Phys. Rev. B* **84** 235416

[35] Zhang J, Wang Y and Wang X 2013 Rough contact is not always bad for interfacial energy coupling *Nanoscale* **5** 11598–603
[36] Zhang J and Wang X 2013 Thermal transport in bent graphene nanoribbons *Nanoscale* **5** 734–43
[37] Zhang J, Hong Y and Yue Y 2015 Thermal transport across graphene and single layer hexagonal boron nitride *Journal of Applied Physics* **117** 134307
[38] Chenebuah E T, Nganbe M and Tchagang A B 2021 Comparative analysis of machine learning approaches on the prediction of the electronic properties of perovskites: a case study of ABX(3) and A(2)BB'X-6 *Mater. Today Commun.* **27** 102462
[39] Ford E, Maneparambil K, Rajan S and Neithalath N 2021 Machine learning-based accelerated property prediction of two-phase materials using microstructural descriptors and finite element analysis *Comput. Mater. Sci.* **191** 110328
[40] Hosokawa H, Calvert E L and Shimojima K 2021 Machine learning prediction for magnetic properties of Sm-Fe-N based alloys produced by melt spinning *J. Magn. Magn. Mater.* **526** 167651
[41] Jiang Y, Chen D, Chen X, Li T Y, Wei G W and Pan F 2021 Topological representations of crystalline compounds for the machine-learning prediction of materials properties *NPJ Comput. Mater.* **7** 28
[42] Qin J C, Liu Z F, Ma M S, Liu F, Qi Z M and Li Y X 2021 Structure and microwave dielectric properties of gillespite-type ACuSi(4)O(10) (A = Ca, Sr, Ba) ceramics and quantitative prediction of the Q x f value via machine learning *ACS Appl. Mater. Interfaces* **13** 17817–26
[43] Tran H D *et al* 2020 Machine-learning predictions of polymer properties with polymer genome *J. Appl. Phys.* **128** 171104
[44] Belle C E, Aksakalli V and Russo S P 2021 A machine learning platform for the discovery of materials *J. Cheminform.* **13** 42
[45] del Cueto M and Troisi A 2021 Determining usefulness of machine learning in materials discovery using simulated research landscapes *Phys. Chem. Chem. Phys.* **23** 14156–63
[46] Juan Y F, Dai Y B, Yang Y and Zhang J 2021 Accelerating materials discovery using machine learning *J. Mater. Sci. Technol.* **79** 178–90
[47] Kailkhura B, Gallagher B, Kim S, Hiszpanski A and Han T Y J 2019 Reliable and explainable machine-learning methods for accelerated material discovery *NPJ Comput. Mater.* **5** 108
[48] Schleder G R, Focassio B and Fazzio A 2021 Machine learning for materials discovery: two-dimensional topological insulators *Appl. Phys. Rev.* **8** 031409
[49] Tao Q L, Xu P C, Li M J and Lu W C 2021 Machine learning for perovskite materials design and discovery *NPJ Comput. Mater.* **7** 23
[50] DeCarvalho G, Frollini E and DosSantos W N 1996 Thermal conductivity of polymers by hot-wire method *J. Appl. Polym. Sci.* **62** 2281–5
[51] Healy J J, de Groot J J and Kestin J 1976 The theory of the transient hot-wire method for measuring thermal conductivity *Physica B + C* **82** 392–408
[52] Choi T Y, Poulikakos D, Tharian J and Sennhauser U 2005 Measurement of thermal conductivity of individual multiwalled carbon nanotubes by the 3-omega method *Appl. Phys. Lett.* **87** 013108
[53] An X H, Cheng J H, Yin H Q, Xie L D and Zhang P 2015 Thermal conductivity of high temperature fluoride molten salt determined by laser flash technique *Int. J. Heat Mass Transfer* **90** 872–7
[54] Cahill D G 2004 Analysis of heat flow in layered structures for time-domain thermoreflectance *Rev. Sci. Instrum.* **75** 5119–22
[55] Gao J S, Xie D M, Wang X W, Zhang X and Yue Y N 2020 High thermal conductivity of free-standing skeleton in graphene foam *Appl. Phys. Lett.* **117** 251901
[56] Wang R D, Zobeiri H, Xie Y S, Wang X W, Zhang X and Yue Y N 2020 Distinguishing optical and acoustic phonon temperatures and their energy coupling factor under photon excitation in nm 2D materials *Adv. Sci.* **7** 2000097
[57] Jain A and McGaughey A J H 2015 Effect of exchange-correlation on first-principles-driven lattice thermal conductivity predictions of crystalline silicon *Comput. Mater. Sci.* **110** 115–20
[58] Zhang Y, Skoug E, Cain J, Ozoliņš V, Morelli D and Wolverton C 2012 First-principles description of anomalously low lattice thermal conductivity in thermoelectric Cu-Sb-Se ternary semiconductors *Phys. Rev. B* **85** 054306
[59] Donadio D and Galli G 2007 Thermal conductivity of isolated and interacting carbon nanotubes: comparing results from molecular dynamics and the Boltzmann transport equation *Phys. Rev. Lett.* **99** 255502
[60] Chernatynskiy A and Phillpot S R 2010 Evaluation of computational techniques for solving the Boltzmann transport equation for lattice thermal conductivity calculations *Phys. Rev. B* **82** 134301
[61] Romano G, Esfarjani K, Strubbe D A, Broido D and Kolpak A M 2016 Temperature-dependent thermal conductivity in silicon nanostructured materials studied by the Boltzmann transport equation *Phys. Rev. B* **93** 035408
[62] MullerPlathe F 1997 A simple nonequilibrium molecular dynamics method for calculating the thermal conductivity *J. Chem. Phys.* **106** 6082–5

[63] Sellan D P, Landry E S, Turney J E, McGaughey A J H and Amon C H 2010 Size effects in molecular dynamics thermal conductivity predictions *Phys. Rev. B* **81** 214305
[64] Hu J N, Ruan X L and Chen Y P 2009 Thermal conductivity and thermal rectification in graphene nanoribbons: a molecular dynamics study *Nano Lett.* **9** 2730–5
[65] Kurt H and Kayfeci M 2009 Prediction of thermal conductivity of ethylene glycol-water solutions by using artificial neural networks *Appl. Energy* **86** 2244–8
[66] Hearst M A, Dumais S T, Osuna E, Platt J and Scholkopf B 1998 Support vector machines *IEEE Intell. Syst. Appl.* **13** 18–28
[67] Quinlan J R 1986 Induction of decision trees *Mach. Learn.* **1** 81–106
[68] Quinonero-Candela J Q and Rasmussen C E 2005 A unifying view of sparse approximate Gaussian process regression *J. Mach. Learn. Res.* **6** 1939–59
[69] Pelikan M, Goldberg D E and Cantu-Paz E 1999 BOA: The Bayesian optimization algorithm Gecco-99 *Proc. of the Genetic and Evolutionary Computation Conf. pp 525–32*
[70] Seko A, Hayashi H, Nakayama K, Takahashi A and Tanaka I 2017 Representation of compounds for machine-learning prediction of physical properties *Phys. Rev. B* **95** 144110
[71] Raccuglia P, Elbert K C, Adler P D, Falk C, Wenny M B, Mollo A, Zeller M, Friedler S A, Schrier J and Norquist A J 2016 Machine-learning-assisted materials discovery using failed experiments *Nature* **533** 73–6
[72] Hajibabaei A and Kim K S 2021 Universal machine learning interatomic potentials: surveying solid electrolytes *J. Phys. Chem. Lett.* **12** 8115–20
[73] Nikoulis G, Byggmastar J, Kioseoglou J, Nordlund K and Djurabekova F 2021 Machine-learning interatomic potential for W-Mo alloys *J. Phys.: Condens. Matter* **33** 315403
[74] Schran C, Thiemann F L, Rowe P, Muller E A, Marsalek O and Michaelides A 2021 Machine learning potentials for complex aqueous made simple *Proc. Natl Acad. Sci. USA* **118** e2110077118
[75] Wyant S, Rohskopf A and Henry A 2021 Machine learned interatomic potentials for modeling interfacial heat transport in Ge/GaAs *Comput. Mater. Sci.* **200** 110836
[76] Chen C, Zuo Y X, Ye W K, Li X G, Deng Z and Ong S P 2020 A critical review of machine learning of energy materials *Adv. Energy Mater.* **10** 1903242
[77] Schleder G R, Padilha A C M, Acosta C M, Costa M and Fazzio A 2019 From DFT to machine learning: recent approaches to materials science-a review *J. Phys.-Mater.* **2** 032001
[78] Ben Chaabene W, Flah M and Nehdi M L 2020 Machine learning prediction of mechanical properties of concrete: critical review *Constr. Build. Mater.* **260** 119889
[79] Jones D E, Ghandehari H and Facelli J C 2016 A review of the applications of data mining and machine learning for the prediction of biomedical properties of nanoparticles *Comput. Methods Prog. Bio.* **132** 93–103
[80] Liu W X, Zhu Y, Wu Y Q, Chen C, Hong Y, Yue Y A, Zhang J C and Hou B 2021 Molecular dynamics and machine learning in catalysts *Catalysts* **11** 1129
[81] Unke O T, Chmiela S, Sauceda H E, Gastegger M, Poltaysky I, Schutt K T, Tkatchenko A and Muller K R 2021 Machine learning force fields *Chem. Rev.* **121** 10142–86
[82] Luo H B, Xiong C H, Fang W L, Love P E D, Zhang B W and Ouyang X 2018 Convolutional neural networks: computer vision-based workforce activity assessment in construction *Automat. Constr.* **94** 282–9
[83] Hershey S *et al* 2017 CNN architectures for large-scale audio classification *2017 IEEE International Conference on Acoustics, Speech and Signal Processing (ICASSP)* 131–5
[84] Kamilaris A and Prenafeta-Boldu F X 2018 A review of the use of convolutional neural networks in agriculture *J. Agri. Sci.* **156** 312–22
[85] Rao C P and Liu Y 2020 Three-dimensional convolutional neural network (3D-CNN) for heterogeneous material homogenization *Comput. Mater. Sci.* **184** 109850
[86] Lorena G, Robinson G, Stefania P, Pasquale C, Fabiano B and Franco M 2019 Automatic microstructural classification with convolutional neural network *Adv. Intell. Syst. Comp.* **884** 170–81
[87] Warmuzek M, Zelawski M and Jalocha T 2021 Application of the convolutional neural network for recognition of the metal alloys microstructure constituents based on their morphological characteristics *Comput. Mater. Sci.* **199** 110722
[88] Kitaguchi D *et al* 2020 Real-time automatic surgical phase recognition in laparoscopic sigmoidectomy using the convolutional neural network-based deep learning approach *Surg. Endosci.* **34** 4924–31
[89] Noble W S 2006 What is a support vector machine ? *Nat. Biotechnol.* **24** 1565–7
[90] Tersoff J 1988 Empirical interatomic potential for silicon with improved elastic properties *Phys. Rev. B* **38** 9902–5
[91] Tersoff J 1988 Empirical interatomic potential for carbon, with applications to amorphous-carbon *Phys. Rev. Lett.* **61** 2879–82
[92] Lindsay L and Broido D A 2010 Optimized Tersoff and Brenner empirical potential parameters for lattice dynamics and phonon thermal transport in carbon nanotubes and graphene *Phys. Rev. B* **82** 205441

[93] Brenner D W, Shenderova O A, Harrison J A, Stuart S J, Ni B and Sinnott S B 2002 A second-generation reactive empirical bond order (REBO) potential energy expression for hydrocarbons *J. Phys.: Condens. Matter* **14** 783–802

[94] Hu W Y, Shu X L and Zhang B W 2002 Point-defect properties in body-centered cubic transition metals with analytic EAM interatomic potentials *Comput. Mater. Sci.* **23** 175–89

[95] van Duin A C T, Dasgupta S, Lorant F and Goddard W A 2001 ReaxFF: a reactive force field for hydrocarbons *J. Phys. Chem. A* **105** 9396–409

[96] Senftle T P *et al* 2016 The ReaxFF reactive force-field: development, applications and future directions *NPJ Comput. Mater.* **2** 15011

[97] Chenoweth K, van Duin A C T and Goddard W A 2008 ReaxFF reactive force field for molecular dynamics simulations of hydrocarbon oxidation *J. Phys. Chem. A* **112** 1040–53

[98] Martinez J A, Yilmaz D E, Liang T, Sinnott S B and Phillpot S R 2013 Fitting empirical potentials: Challenges and methodologies *Curr. Opin. Solid. Solid State Mater. Sci.* **17** 263–70

[99] Shchygol G, Yakovlev A, Trnka T, van Duin A C T and Verstraelen T 2019 ReaxFF parameter optimization with monte-carlo and evolutionary algorithms: guidelines and insights *J. Chem. Theory Comput.* **15** 6799–812

[100] Larsson H R, van Duin A C T and Hartke B 2013 Global optimization of parameters in the reactive force field ReaxFF for SiOH *J. Comput. Chem.* **34** 2178–89

[101] Zhang L, Han J, Wang H, Car R and E Weinan 2018 Deep potential molecular dynamics: a scalable model with the accuracy of quantum mechanics *Phys. Rev. Lett.* **120** 143001

[102] Behler J and Parrinello M 2007 Generalized neural-network representation of high-dimensional potential-energy surfaces *Phys. Rev. Lett.* **98** 146401

[103] Bartok A P, Payne M C, Kondor R and Csanyi G 2010 Gaussian approximation potentials: the accuracy of quantum mechanics, without the electrons *Phys. Rev. Lett.* **104** 136403

[104] Shapeev A V 2016 Moment Tensor Potentials: A Class of Systematically Improvable Interatomic Potentials *Multiscale Model Sim.* **14** 1153–73

[105] Wang H, Zhang L F, Han J Q and E Weinan 2018 DeePMD-kit: A deep learning package for many-body potential energy representation and molecular dynamics *Comput. Phys. Commun.* **228** 178–84

[106] Bartok A P and Csanyi G 2015 Gaussian approximation potentials: A brief tutorial introduction *Int. J. Quantum Chem.* **115** 1051–7

[107] Plimpton S 1995 Fast parallel algorithms for short-range molecular-dynamics *J. Comput. Phys.* **117** 1–19

[108] Balyakin I A, Rempel S V, Ryltsev R E and Rempel A A 2020 Deep machine learning interatomic potential for liquid silica *Phys. Rev. E* **102** 052125

[109] Jia W *et al* 2020 Pushing the Limit of Molecular Dynamics with Ab Initio Accuracy to 100 Million Atoms with Machine Learning *SC20: International Conference for High Performance Computing, Networking, Storage and Analysis* 1–14

[110] Pan X L, Yang J J, Van R, Epifanovsky E, Ho J M, Huang J, Pu J Z, Mei Y, Nam K and Shao Y H 2021 Machine-learning-assisted free energy simulation of solution-phase and enzyme reactions *J. Chem. Theory Comput.* **17** 5745–58

[111] Wen T Q *et al* 2019 Development of a deep machine learning interatomic potential for metalloid-containing Pd-Si compounds *Phys. Rev. B* **100** 174101

[112] Fan Z Y, Zeng Z Z, Zhang C Z, Wang Y Z, Song K K, Dong H K, Chen Y and Nissila T A 2021 Neuroevolution machine learning potentials: Combining high accuracy and low cost in atomistic simulations and application to heat transport *Phys. Rev. B* **104** 104309

[113] Fan Z Y, Chen W, Vierimaa V and Harju A 2017 Efficient molecular dynamics simulations with many-body potentials on graphics processing units *Comput. Phys. Commun.* **218** 10–6

[114] Fan Z Y, Pereira L F C, Wang H Q, Zheng J C, Donadio D and Harju A 2015 Force and heat current formulas for many-body potentials in molecular dynamics simulations with applications to thermal conductivity calculations *Phys. Rev. B* **92** 094301

[115] De S, Bartok A P, Csanyi G and Ceriotti M 2016 Comparing molecules and solids across structural and alchemical space *Phys. Chem. Chem. Phys.* **18** 13754–69

[116] Rowe P, Csányi G, Alfè D and Michaelides A 2018 Development of a machine learning potential for graphene *Phys. Rev. B* **97** 054303

[117] Walsh S M, Malouin B A, Browne E A, Bagnall K R, Wang E N and Smith J P 2019 Embedded microjets for thermal management of high power-density electronic devices *IEEE Trans. Compon. Packag. Manuf. Technol.* **9** 269–78

[118] Soleimanzadeh R, Khadar R A, Naamoun M, van Erp R and Matioli E 2019 Near-junction heat spreaders for hot spot thermal management of high power density electronic devices *J. Appl. Phys.* **126** 165113

[119] McGlen R J, Jachuck R and Lin S 2004 Integrated thermal management techniques for high power electronic devices *Appl. Therm. Eng.* **24** 1143–56

[120] Tao P, Shang W, Song C Y, Shen Q C, Zhang F Y, Luo Z, Yi N, Zhang D and Deng T 2015 Bioinspired engineering of thermal materials *Adv. Mater.* **27** 428–63

[121] Liu X J and Rao Z H 2020 A molecular dynamics study on heat conduction of crosslinked epoxy resin based thermal interface materials for thermal management *Comput. Mater. Sci.* **172** 109298

[122] Narayana S and Sato Y 2012 Heat flux manipulation with engineered thermal materials *Phys. Rev. Lett.* **108** 214303
[123] Yan C Z, Yang Y and Wang G 2021 A new 2D continuous-discontinuous heat conduction model for modeling heat transfer and thermal cracking in quasi-brittle materials *Comput. Geotech.* **137** 104231
[124] Zhao L D, He J Q, Berardan D, Lin Y H, Li J F, Nan C W and Dragoe N 2014 BiCuSeO oxyselenides: new promising thermoelectric materials *Energy Environ. Sci.* **7** 2900–24
[125] Qiu P F, Shi X and Chen L D 2016 Cu-based thermoelectric materials *Energy Storage Mater.* **3** 85–97
[126] Yakout M, Elbestawi M A, Veldhuis S C and Nangle-Smith S 2020 Influence of thermal properties on residual stresses in SLM of aerospace alloys *Rapid Prototyping J.* **26** 213–22
[127] Doty J, Yerkes K, Byrd L, Murthy J, Alleyne A, Wolff M, Heister S and Fisher T S 2017 Dynamic Thermal Management for Aerospace Technology: Review and Outlook *J. Thermophys. Heat Trans.* **31** 86–98
[128] Liang Z and Keblinski P 2014 Finite-size effects on molecular dynamics interfacial thermal-resistance predictions *Phys. Rev. B* **90** 075411
[129] Volz S G and Chen G 1999 Molecular dynamics simulation of thermal conductivity of silicon nanowires *Appl. Phys. Lett.* **75** 2056–8
[130] Otey C R, Lau W T and Fan S H 2010 Thermal rectification through vacuum *Phys. Rev. Lett.* **104** 154301
[131] Yang N, Zhang G and Li B W 2009 Thermal rectification in asymmetric graphene ribbons *Appl. Phys. Lett.* **95** 033107
[132] Iijima S 2002 Carbon nanotubes: past, present, and future *Physica* B **323** 1–5
[133] Qin L C, Zhao X L, Hirahara K, Miyamoto Y, Ando Y and Iijima S 2000 The smallest carbon nanotube *Nature* **408** 50
[134] Yamada T, Namai T, Hata K, Futaba D N, Mizuno K, Fan J, Yudasaka M, Yumura M and Iijima S 2006 Size-selective growth of double-walled carbon nanotube forests from engineered iron catalysts *Nat. Nanotechnol.* **1** 131–6
[135] Castro Neto A H, Guinea F, Peres N M R, Novoselov K S and Geim A K 2009 The electronic properties of graphene *Rev. Mod. Phys.* **81** 109–62
[136] Ferrari A C *et al* 2006 Raman spectrum of graphene and graphene layers *Phys. Rev. Lett.* **97** 187401
[137] Meyer J C, Geim A K, Katsnelson M I, Novoselov K S, Booth T J and Roth S 2007 The structure of suspended graphene sheets *Nature* **446** 60–3
[138] Zhang J, Wang X and Xie H 2013 Phonon energy inversion in graphene during transient thermal transport *Phys. Lett. A* **377** 721–6
[139] Zhang J, Wang X and Xie H 2013 Co-existing heat currents in opposite directions in graphene nanoribbons *Phys. Lett.* A **377** 2970–8
[140] Zhang J, Xu F, Hong Y, Xiong Q and Pan J 2015 A comprehensive review on the molecular dynamics simulation of the novel thermal properties of graphene *RSC Adv.* **5** 89415–26
[141] Wei H, Bao H and Ruan X L 2020 Genetic algorithm-driven discovery of unexpected thermal conductivity enhancement by disorder *Nano Energy* **71** 104619
[142] Braginsky L, Shklover V, Witz G and Bossmann H P 2007 Thermal conductivity of porous structures *Phys. Rev B* **75** 094301
[143] Niu D and Gao H T 2021 Thermal conductivity of ordered porous structures coupling gas and solid phases: a molecular dynamics study *Materials* **14** 2221
[144] Wang N Q, Kaur I, Singh P and Li L K 2021 Prediction of effective thermal conductivity of porous lattice structures and validation with additively manufactured metal foams *Appl. Therm. Eng.* **187** 116558
[145] Wei H, Bao H and Ruan X L 2020 Machine learning prediction of thermal transport in porous media with physics-based descriptors *Int. J. Heat Mass Transfer* **160** 120176
[146] Chen L H, Tran H, Batra R, Kim C and Ramprasad R 2019 Machine learning models for the lattice thermal conductivity prediction of inorganic materials *Comput. Mater. Sci.* **170** 109155
[147] Wu Y J, Fang L and Xu Y B 2019 Predicting interfacial thermal resistance by machine learning *NPJ Comput. Mater.* **5** 56
[148] Liu Z, Yang X, Zhang B and Li W 2021 High thermal conductivity of wurtzite boron arsenide predicted by including four-phonon scattering with machine learning potential acs *Appl. Mater. Interfaces* **13** 53409–15
[149] Eriksson F, Fransson E and Erhart P 2019 The hiphive package for the extraction of high-order force constants by machine learning *Adv. Theor. Simul.* **2** 1800184
[150] Liu Y B, Yang J Y, Xin G M, Liu L H, Csanyi G and Cao B Y 2020 Machine learning interatomic potential developed for molecular simulations on thermal properties of beta-Ga2O3 *J. Chem. Phys.* **153** 144501
[151] Li R Y, Liu Z Y, Rohskopf A, Gordiz K, Henry A, Lee E and Luo T F 2020 A deep neural network interatomic potential for studying thermal conductivity of beta-Ga2O3 *Appl. Phys. Lett.* **117** 152102
[152] Chen C T, Nagao S, Zhang H, Jiu J T, Sugahara T, Suganuma K, Iwashige T, Sugiura K and Tsuruta K 2017 Mechanical deformation of sintered porous Ag Die attach at high

temperature and its size effect for wide-bandgap power device design *J. Electron. Mater.* **46** 1576–86
[153] Hsu P I, Huang M, Xi Z, Wagner S, Suo Z and Sturm J C 2004 Spherical deformation of compliant substrates with semiconductor device islands *J. Appl. Phys.* **95** 705–12
[154] Smit B and Maesen T L M 2008 Molecular simulations of zeolites: adsorption, diffusion, and shape selectivity *Chem. Rev.* **108** 4125–84
[155] Siriwardane R V, Shen M S and Fisher E P 2005 Adsorption of CO2 on zeolites at moderate temperatures *Energ Fuel* **19** 1153–9
[156] Montanari T and Busca G 2008 On the mechanism of adsorption and separation of CO2 on LTA zeolites: an IR investigation *Vib. Spectrosc.* **46** 45–51
[157] Palomino M, Corma A, Rey F and Valencia S 2010 New insights on CO2-methane separation using LTA zeolites with different Si/Al ratios and a first comparison with MOFs *Langmuir* **26** 1910–7
[158] Morris R E and Wheatley P S 2008 Gas storage in nanoporous materials *Angew. Chem. Int. Ed.* **47** 4966–81
[159] Simon C M, Kim J, Lin L C, Martin R L, Haranczyk M and Smit B 2014 Optimizing nanoporous materials for gas storage *Phys. Chem. Chem. Phys.* **16** 5499–513
[160] Evans J D and Couder F X 2017 Predicting the mechanical properties of zeolite frameworks by machine learning *Chem. Mater.* **29** 7833–9
[161] Deng Y P, Du T and Li H 2021 Relationship of structure and mechanical property of silica with enhanced sampling and machine learning *J. Am. Ceram. Soc.* **104** 3910–20
[162] Zhang Z S, Hong Y, Hou B, Zhang Z T, Negahban M and Zhang J C 2019 Accelerated discoveries of mechanical properties of graphene using machine learning and high-throughput computation *Carbon* **148** 115–23
[163] Mortazavi B, Silani M, Podryabinkin E V, Rabczuk T, Zhuang X Y and Shapeev A V 2021 First-principles multiscale modeling of mechanical properties in graphene/borophene heterostructures empowered by machine-learning interatomic potentials *Adv. Mater.* **33** 2102807
[164] Liu Y, Zhao T L, Ju W W and Shi S Q 2017 Materials discovery and design using machine learning *J. Materiomics* **3** 159–77
[165] Saal J E, Oliynyk A O and Meredig B 2020 Machine learning in materials discovery: confirmed predictions and their underlying approaches *Annu. Rev. Mater. Res.* **50** 49–69
[166] Xiong Z, Cui Y X, Liu Z H, Zhao Y, Hu M and Hu J J 2020 Evaluating explorative prediction power of machine learning algorithms for materials discovery using k-fold forward cross-validation *Comput. Mater. Sci.* **171** 109203
[167] Zhou Q, Tang P Z, Liu S X, Pan J B, Yan Q M and Zhang S C 2018 Learning atoms for materials discovery *Proc. Natl Acad. Sci. USA* **115** E6411–7
[168] Alam H and Ramakrishna S 2013 A review on the enhancement of figure of merit from bulk to nano-thermoelectric materials *Nano Energy* **2** 190–212
[169] Sundarraj P, Maity D, Roy S S and Taylor R A 2014 Recent advances in thermoelectric materials and solar thermoelectric generators - a critical review *RSC Adv.* **4** 46860–74
[170] Han D, Yang X H, Du M, Xin G M, Zhang J C, Wang X Y and Cheng L 2021 Improved thermoelectric properties of WS2-WSe2 phononic crystals: insights from first-principles calculations *Nanoscale* **13** 7176–92
[171] Xin J W, Basit A, Li S H, Danto S, Tjin S C and Wei L 2021 Inorganic thermoelectric fibers: a review of materials, fabrication methods, and applications *Sensors* **21** 3437
[172] Li B L and Chen K Q 2017 Effects of electron-phonon interactions on the spin-dependent Seebeck effect in graphene nanoribbons *Carbon* **119** 548–54
[173] Lu P X, Shen Z G and Hu X 2010 Electronic structure of the thermoelectric materials PbTe and AgPb18SbTe20 from first-principles calculations *J. Mater. Res.* **25** 1030–6
[174] Hou Z F, Takagiwa Y, Shinohara Y, Xu Y B and Tsuda K 2019 machine-learning-assisted development and theoretical consideration for the Al2Fe3Si3 thermoelectric material *ACC Appl. Mater. Interfaces* **11** 11545–54
[175] Iwasaki Y *et al* 2019 Machine-learning guided discovery of a new thermoelectric material *Sci. Rep.* **9** 2751
[176] Gaultois M W, Oliynyk A O, Mar A, Sparks T D, Mulholland G J and Meredig B 2016 Perspective: Web-based machine learning models for real-time screening of thermoelectric materials properties *APL Mater.* **4** 053213